Advances in Modelling and Analysis A
Vol. 55, No. 3, September, 2018, pp. 99-107
Journal homepage: http://iieta.org/Journals/AMA/AMA_A

Linear Fresnel plant with primary reflectors movable around two axes

Mario A. Cucumo[1*], Vittorio Ferraro[1], Dimitrios Kaliakatsos[1], Marilena Mele[2], Francesco Nicoletti[1]

[1] DIMEG, Università della Calabria, Via P. Bucci 87036 Rende (CS), Italy
[2] Freelance

Corresponding Author Email: mario.cucumo@unical.it

https://doi.org/10.18280/ama_a.550301

Received: 16 February 2018
Accepted: 3 May 2018

Keywords:
concentrating solar power, linear Fresnel, bi-axial tracking system, law of motion

ABSTRACT

In Linear Fresnel solar concentration systems there are some energy losses due to the arrangement of the primary reflectors. An important loss of geometric type is caused by the fact that mirrors have only one degree of freedom. Therefore, the accuracy of the solar tracking, at the ends of the collector, cannot be guaranteed, especially if the height of the absorber tube is considerable. The problem could be solved by making the primary reflectors placed at the ends of the plant movable around two axes. In the work, the mathematical law is analytically obtained to determine the position that each reflectors must assume during the day. The study shows that they must be moved independently in each direction. For the purposes of reducing the cost of the plant, a configuration is studied in which, around an axis, the reflectors are moved with the same motor, differentiating the movement only around the other axis of rotation. Thanks to the presence of the secondary reflector, the tracking error committed is not significant.
Finally, the advantages, in terms of performance, obtained with the adoption of the above-mentioned reflectors, both for North-South oriented plants and for East-West oriented plants, are illustrated.

1. INTRODUCTION

Concentrated solar collectors with Fresnel reflectors are composed of flat mirrors that reflect solar radiation to a fixed receiver parallel to the mirrors. The receiver consists of an absorber tube, inside which flows the heat-transfer fluid which absorbs the incident energy. It can be used for the production of electricity or for industrial applications, as well as other plants that use renewable sources [1-2]. The plant can also be equipped with a thermal storage tank, necessary to compensate for moments of absence or poor insolation.

The working fluid can be diathermic oil or a mixture of molten salts or water for direct steam production. Above the absorber tube there is the secondary reflector which refocuses the rays, possibly reflected with slight errors, directing the rays towards the tube. The primary reflectors are equipped with one degree of freedom: the rotation around the axis parallel to the receiver tube. The use of only flat mirrors reduces the initial installation costs compared to the use of more complex geometries.

The work presents an innovative technique to be used in Fresnel linear systems. This technique allows some problems related to the movement of the mirrors around a single axis to be solved. In particular, to reduce some optical energy losses that occur inevitably in the longitudinal ends of the system, a configuration has been studied in which the mirrors placed at the ends have two degrees of freedom. The mathematical law will be obtained, analytically, to know the position that these new reflectors must assume at every moment of the day. The strengths and weaknesses of this system solution are analyzed, proposing solutions regarding the reduction of initial costs and the increase of the overall efficiency of the collector.

2. ORIENTATION OF PRIMARY REFLECTORS FOR SINGLE-AXIS TRACKING SYSTEMS

A feature that distinguishes Fresnel reflector systems compared to other solar concentration technologies is the best exploitation of the land on which they are installed; in fact, a small gap between the mirrors is enough to minimize shadowing.

Figure 1 shows the representation of a cross-section of the plant, in which we can see how, with the use of flat mirrors, solar radiation can be effectively concentrated. The reflectors rotate around their longitudinal axis according to the position of the sun on the celestial vault.

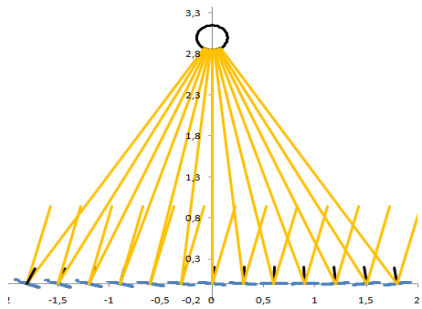

Figure 1. Operating diagram of a linear system of Fresnel

Through spherical trigonometry formulas it is possible to derive the link between the inclination of a generic reflector and the solar coordinates [3]. Indicating with h the height at which the absorber tube is installed with respect to the rotation axis of the mirror, the generic reflector is positioned at a distance D with respect to the projection of the tube on the

horizontal plane (Figure 2). The angle β which forms the normal with the positive direction of the x-axis is given by the following relation:

$$\beta = 90° - \arctan\frac{\sqrt{1-\cos^2\alpha\cos^2 a}-\sin\alpha}{\cos\alpha\sin a}+\frac{1}{2}\arctan\left(\frac{D}{h}\right) \quad (1)$$

where a represents the solar azimuth and α is the solar altitude.

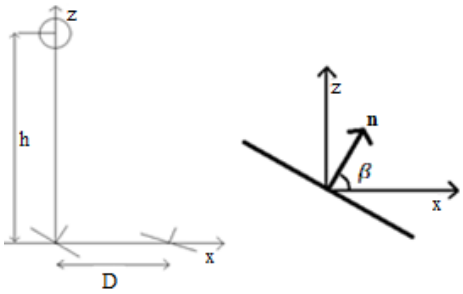

Figure 2. Generic reflector

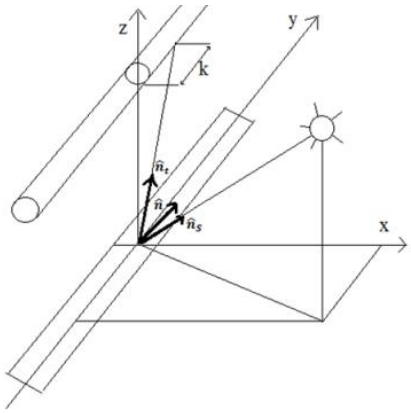

Figure 3. Schematic reflection on a reflecting panel

Figure 3 shows the three characteristic directions of the reflection, indicated respectively by three versors:

- versor $\hat{n}$ is normal to the surface of the mirror; it belongs to the x-z plane because the mirror can rotate only around the y axis;
- versor $\hat{n}_T$ indicates the direction of the reflected beam;
- versor $\hat{n}_S$ indicates the direction from which the sun's rays come and is identified by solar altitude α and azimuth a.

The term *k*, visible in Figure 3, assumes considerable importance [4]. It is representative of the point where the reflected ray affects the absorption system. In fact, the point of arrival on the tube is not on the same cross-section as the point where the reflection takes place. With reference to the final part of the system, it happens that the reflected rays, owing to this shift, do not hit the receiver. The length *k*, therefore, represents the portion of the implant in which the reflecting surfaces do not provide a useful effect. Its value is obtained by resorting still to spherical trigonometry [3]:

$$k = \frac{\cos\alpha\cos a}{\sqrt{1-\cos^2\alpha\cos^2 a}}\cdot\sqrt{D^2+h^2} \quad (2)$$

3. ORIENTATION OF PRIMARY REFLECTORS FOR BIASSIAL TRACKING SYSTEMS

In order to avoid energy dispersion at the ends of the plant, a system with two-degrees-of-freedom tracker was analyzed. Only the reflectors arranged in the end parts of the collector will have biaxial movement. The inclinations that the latter must assume, in order to reflect the radiation exactly at the point of the tube belonging to the same cross-section as the point where the reflection takes place, are calculated below. Figure 4 shows a top view of the sphere enclosing the three versors, for a reflector placed at a distance *D* from the projection of the axis of the tube on the ground. On its outer surface, the points S, N, T are provided by the intersection, respectively, with the sunrays versor, with the normal versor to the reflector surface and with the reflected ray versor. The arcs t and t' represent, respectively, the intersection of the external surface of the sphere with the North-South vertical plane and with the plane passing through the North-South straight line and the tube axis.

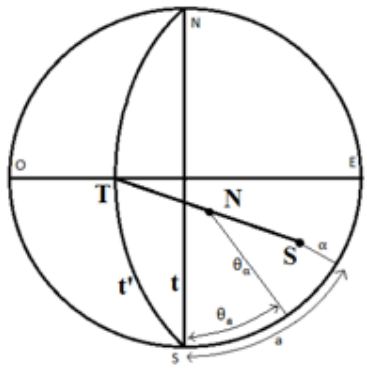

Figure 4. Representation of the sphere from above

With reference to a system arranged in a north-south direction, each row of mirrors must be inclined in such a way that the reflected ray is always incident on the receiving tube within the vertical East-West plane. Versor $\hat{n}_t$ must therefore have coordinates:

$$\hat{n}_t = \left\{\frac{D}{\sqrt{D^2+h^2}};0;\frac{h}{\sqrt{D^2+h^2}}\right\} \quad (3)$$

First of all, it is necessary to determine the apparent motion of the sun with reference to the place of interest. The apparent position of the sun in the celestial vault is identified by the solar altitude **α** and azimuth **a** that can be calculated with the formulas found in the literature [3]. Versor $\hat{n}_S$ has the following coordinates:

$$\hat{n}_S = \{\cos\alpha\sin a;\cos\alpha\cos a;\sin\alpha\} = \{x_S, y_S, z_S\} \quad (4)$$

The position of the normal to the surface of the mirror $\hat{n}$ is defined according to the two parameters θ_α and θ_a (Figure 4) which represent, respectively, the angular height of the normal, with respect to the horizontal plane, and the azimuth of the normal with respect to the South direction.

$$\hat{n} = \{\cos\theta_\alpha\sin\theta_a;\cos\theta_\alpha\cos\theta_a;\sin\theta_\alpha\} \quad (5)$$

The values of these two parameters are defined by imposing two conditions (the two laws of reflection):

- the three versors belong to the same plane π;
- the angle formed by $\hat{n}$ and $\hat{n}_t$ and that formed by $\hat{n}$ and $\hat{n}_s$ are congruent.

The π plane passes through the origin of the axes, for which it presents an equation like:

$$z = a_1 \cdot x + a_2 \cdot y \tag{6}$$

The constants a_1 and a_2 are determined by imposing that the plane passes through points S and T:

$$\begin{cases} h = a_1 \cdot D \\ z_S = a_1 \cdot x_S + a_2 \cdot y_S \end{cases} \tag{7}$$

from which it is obtained:

$$\pi : z = \frac{h}{D} \cdot x + \frac{D \cdot z_S - h \cdot x_S}{D \cdot y_S} \cdot y \tag{8}$$

To respect the first condition, therefore, it is necessary that point N belongs to the π plan:

$$\tan\theta_\alpha = \frac{h}{D} \cdot \sin\theta_a + \frac{D \cdot z_S - h \cdot x_S}{D \cdot y_S} \cdot \cos\theta_a \tag{9}$$

The second condition, however, requires the equality between the values of the product scalar between $\hat{n}$ and $\hat{n}_t$ and between $\hat{n}$ and $\hat{n}_s$:

$$x_S \cos\theta_\alpha \sin\theta_a + y_S \cos\theta_\alpha \cos\theta_a + z_S \sin\theta_\alpha = \\ = \frac{\cos\theta_\alpha \sin\theta_a D}{\sqrt{D^2 + h^2}} + \frac{\sin\theta_\alpha h}{\sqrt{D^2 + h^2}} \tag{10}$$

The Eq. (9) and (10) represent a system of equations in the two unknowns θ_α and θ_a. The analytical solution, as far as the azimuth of the surface is concerned, is as follows:

$$\theta_a = \arctan \frac{\frac{h(D \cdot z_S - h \cdot x_S)}{\sqrt{D^2 + h^2}} - D\left(y_S^2 + z_S^2\right) + x_S z_S h}{D \cdot x_S y_S + h \cdot y_S z_S - y_S \sqrt{D^2 + h^2}} \tag{11}$$

Since, as is known, the arctangent function provides values between -π/2 and π/2, to take into account all the solutions it is necessary to make a correction:

$$\theta_{ac} = \theta_a - \text{sign}(\theta_a) \cdot \pi \qquad \text{if } |a| > \pi/2 \tag{12}$$

The expression of θ_α is, instead, the following:

$$\theta_\alpha = \arctan\left(\frac{h}{D} \cdot \frac{\theta_{ac}}{\sqrt{1+\theta_{ac}^2}} + \frac{D \cdot z_S - h \cdot x_S}{D \cdot y_S} \cdot \frac{1}{\sqrt{1+\theta_{ac}^2}} \right) \tag{13}$$

4. ROTATION ANGLE OF THE REFLECTORS

Eq. (12) and (13) provide information on the inclination of the reflectors according to the solar altitude, azimuth and the position with respect to the tube. The movement system chosen to allow the normal to follow the specified trajectory must have two degrees of freedom. Two independent rotations must therefore guarantee, instant by instant, the correctness of the position of the normal versor.

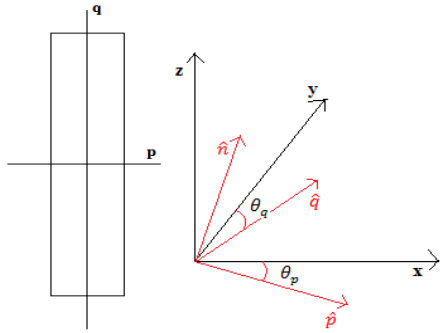

Figure 5. Frame attached to reflector and absolute frame

With reference to Figure 5, lines *p* and *q* have been defined, which respectively indicate the transverse and longitudinal axes passing through the center of the reflector. The frame of the panel is, therefore, composed of the three versors $\hat{p}$, $\hat{q}$ (which lie respectively on the lines *p* and *q*) and $\hat{n}$ (perpendicular to both). The coordinates of the versor $\hat{p}$ and $\hat{q}$ are indicated as follows:

$$\hat{p} = \{x_P, y_P, z_P\} \\ \hat{q} = \{x_q, y_q, z_q\} \tag{14}$$

In the reference configuration of the reflector, this frame coincides with the fixed one. Knowing, therefore, the direction of the normal, the two rotation axes must be identified. The solution consists in performing a primary rotation around the *y* axis, of an angle θ_p, and a secondary rotation around the *p* axis, by an angle θ_q.

The angle θ_p defines the rotation of versor $\hat{p}$ with respect to the *x* axis, around the *y* axis. Versor $\hat{n}$ is uniquely determined because it belongs to the intersection of the *x*-*z* plane (the primary rotation occurs around the *y*-axis) and the plane perpendicular to the normal versor $\hat{n}$. Therefore, for the first condition:

$$y_P = 0 \tag{15}$$

The second condition implies that the dot product between $\hat{p}$ and $\hat{n}$ must be null:

$$x_P \cos\theta_\alpha \sin\theta_{ac} + z_P \sin\theta_\alpha = 0 \tag{16}$$

From this last equation:

$$\theta_P = \arctan\frac{z_P}{x_P} = \arctan\left(-\frac{\sin\theta_{ac}}{\tan\theta_\alpha} \right) \tag{17}$$

and, so:

$$\begin{cases} x_P = \cos\theta_P \\ y_P = 0 \\ z_P = \sin\theta_P \end{cases} \tag{18}$$

The angle θ_q, on the other hand, is generated by a rotation around the p axis: it, therefore, represents the angle between the y and q axes. The direction of the q-axis is defined by versor $\hat{q}$, which is perpendicular to both the normal versor $\hat{n}$ and versor $\hat{p}$:

$$\hat{q} = \hat{n} \times \hat{p} \tag{19}$$

from which:

$$\hat{q} = \det\begin{bmatrix} \hat{i} & \hat{j} & \hat{k} \\ \cos\theta_\alpha \sin\theta_{ac} & \cos\theta_\alpha \cos\theta_{ac} & \sin\theta_\alpha \\ \cos\theta_P & 0 & \sin\theta_P \end{bmatrix} \tag{20}$$

The components are, therefore:

$$\hat{q} = \begin{cases} x_q = \cos\theta_\alpha \cos\theta_{ac} \sin\theta_P \\ y_q = \sin\theta_\alpha \cos\theta_P - \cos\theta_\alpha \sin\theta_{ac} \sin\theta_P \\ z_q = -\cos\theta_\alpha \cos\theta_{ac} \cos\theta_P \end{cases} \tag{21}$$

Angle θ_q is:

$$\theta_q = \mathrm{sgn}(z_q) \cdot \arctan\frac{\sqrt{x_q^2 + z_q^2}}{y_q} \tag{22}$$

It is considered positive if the rotation around the p axis occurs in an anti-clockwise direction. After some mathematical steps, it results:

$$\theta_q = -\arcsin(\cos\theta_\alpha \cos\theta_{ac}) \tag{23}$$

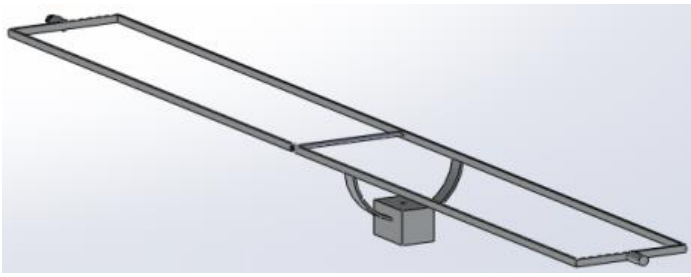

Figure 6. Panel support for bi-axial movement

The movement system used to allow the two rotations is shown in Figure 6. The entire support of the panel can rotate around the longitudinal axis; the servomotor, which moves the panel around the secondary axis, also integrally rotates with the support.

5. ANALYSIS OF RESULTS

With reference to a plant located at a latitude of 40 ° N, oriented in the North-South direction, the trends of the angles of rotation θ_p and θ_q are presented for the summer solstice (Figures 7 and 8) and the winter solstice (Figures 9 and 10).

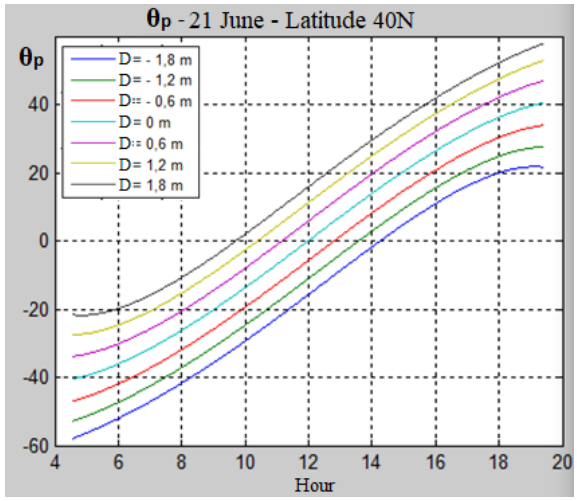

Figure 7. θ_p- June 21 – North-South

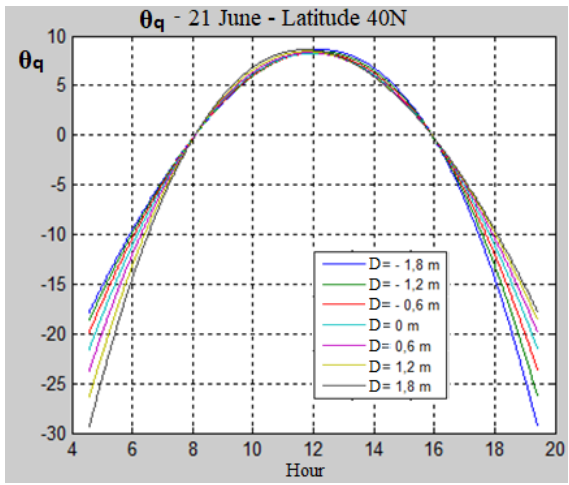

Figure 8. θ_q- June 21–North-South

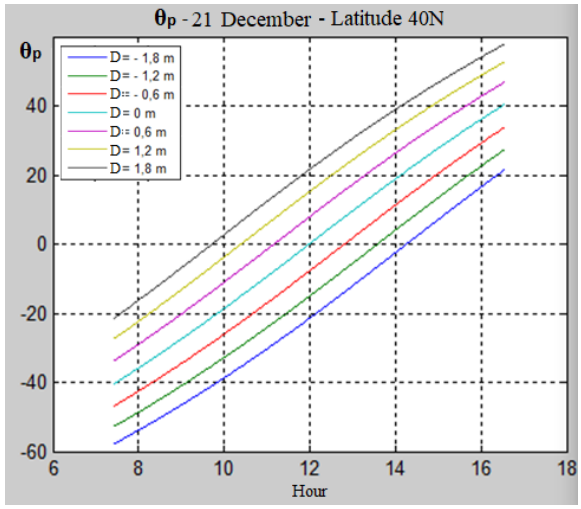

Figure 9. θ_p- December 21 – North-South

During the other days of the year the curves show intermediate trends with respect to these two operating limit conditions. The Figures shown refer to a plant with reflectors spaced 0.6 m apart from each other and a height of the receiving tube of 3 m.

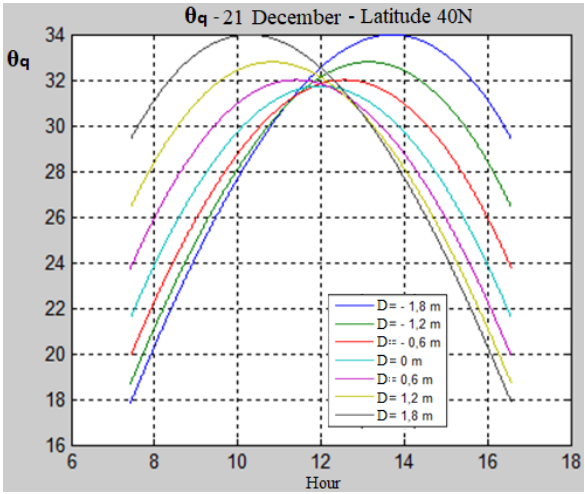

Figure 10. θ_q - December 21 – North-South

The different reflectors do not rotate at the same angles during the day, around either of the two axes. It is therefore necessary to use two independent motors for each reflector. This system solution allows the following error related to the reflectors placed at the ends of the system to be cancelled. However, using two servomotors for each reflector causes a substantial increase in the initial cost of the collector, making it impractical from an economic point of view.

It is observed, however, that the trends of θ_p for the various reflectors are very similar to each other during the day. Therefore, by accepting a minimum error, it is possible to move the reflectors around the p axis with the same servomotor, adopting the law of motion of the central reflector. Rotations of rows of mirrors must be offset by an angle according to their position relative to the tube. The determination of the phase shift angle must be made in such a way that the error committed is minimal.

The generic reflector, moreover, revolves around the q axis with its own law of motion defined by the trend of θ_q.

Reflected beam $\hat{n}_{t,real}$, in this new system configuration, does not affect the pipe exactly (Figure 11). Therefore, it is necessary to estimate the extent of the tracking error 'e' that is committed.

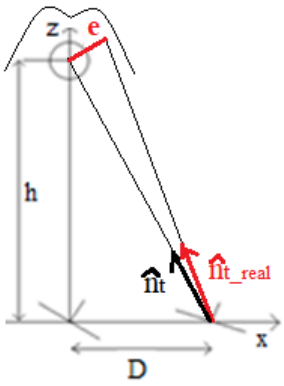

Figure 11. Tracking error

The error '**e**' is calculated with the following equation:

$$e = \hat{e} \cdot \sqrt{D^2 + h^2} \tag{24}$$

where $\hat{e}$ is the angle between $\hat{n}_t$ and $\hat{n}_{t,real}$.

The rays that do not hit the receiver are however refocused towards the tube thanks to the secondary reflector. It has been observed, after numerous attempts, that there is not a single shift angle value that makes errors minimal during the whole year:

- Increasing the shift angle, the error in summer increases and in winter reduces;
- Reducing the shift angle, the error in summer reduces and increases in winter.

For optimal operation, therefore, the shift angle of the reflectors with respect to the central reflector must be changed twice a year. Figure 12 shows the error for June 21, representative of the summer operating conditions. In particular, the shift angle used is shown by the following relation:

$$\theta_P(D) = \theta_P(D=0) + 0.50 \arctan\frac{D}{h} \tag{25}$$

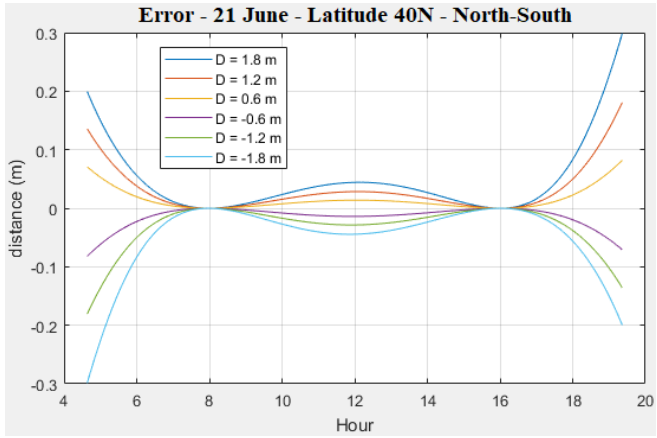

Figure 12. Tracking error- June 21 – North-South

In Figure 13, instead, the error is shown for December 21, representative of the winter conditions. The shift angle is shown by the relation:

$$\theta_P(D) = \theta_P(D=0) + 0.65 \arctan\frac{D}{h} \tag{26}$$

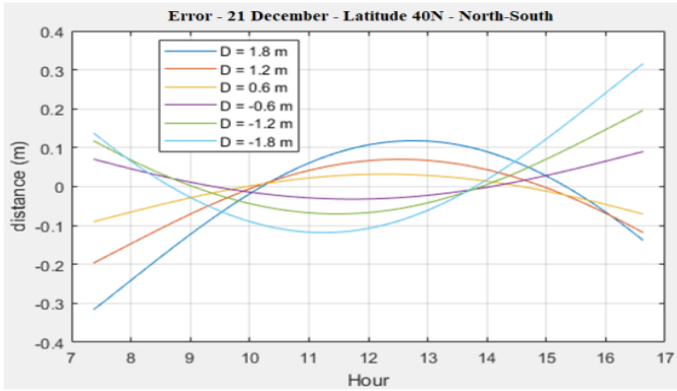

Figure 13. Tracking error- December 21 - North-South

Therefore, changing the shift angle of the lateral reflectors twice a year, the tracking error is almost always reported at values lower than 0.10 m. This means that, to collect the entire reflected radiation, the secondary reflector to be installed above the pipe must have an aperture area at least 0.20 m greater than the diameter of the absorber tube.

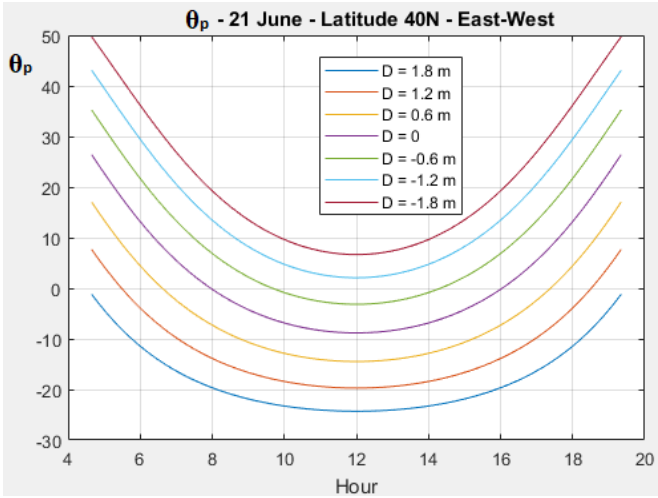

Figure 14. θ_q- June 21 – East-West

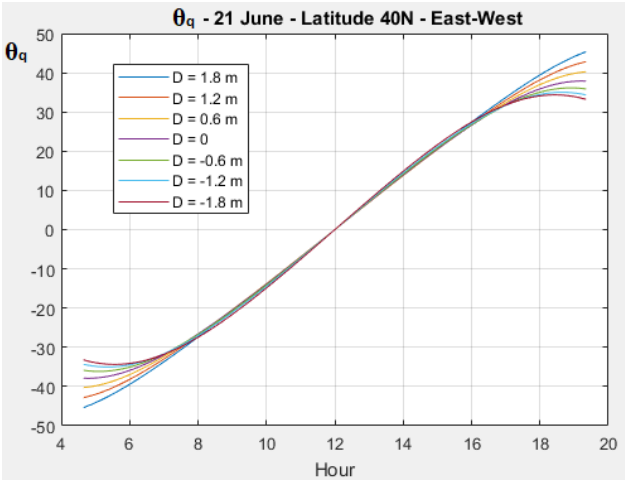

Figure 15. θ_q- June 21 – East-West

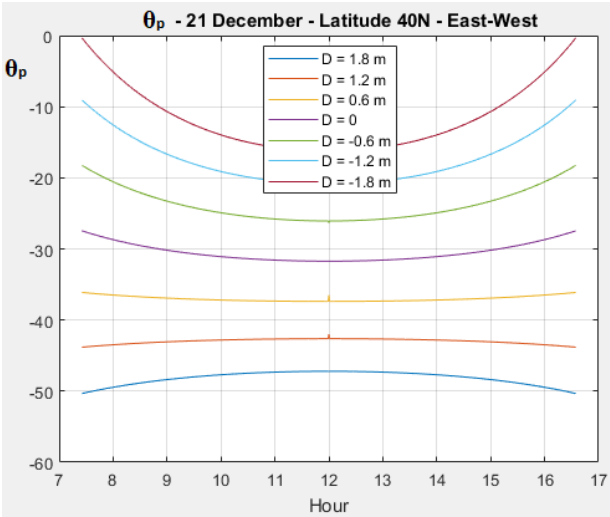

Figure 16. θ_p- December 21 – East-West

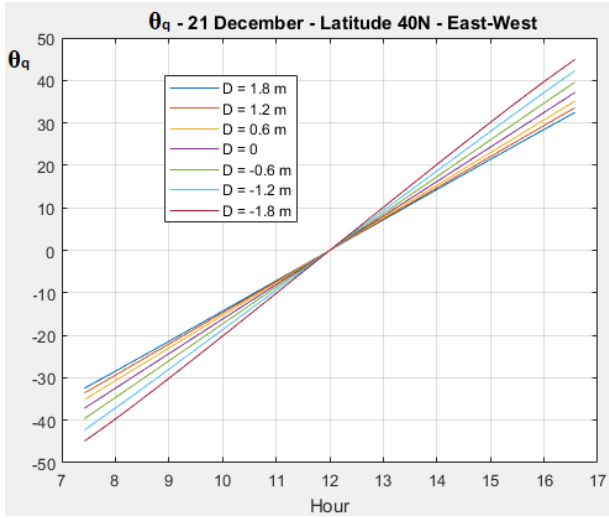

Figure 17. θ_q- December 21– East-West

It is possible to extend the validity of the equations also to the case in which the orientation is East-West. For this purpose a mathematical artifice is used which consists in changing the value of the solar azimuth by 90°. In this way, instead of rotating the orientation of the system, with relative modifications to be made to the equations, the solar trajectory is fictitiously rotated, modifying only the azimuth value. The trends of θ_p and θ_q angles during the summer solstice and the winter solstice are shown in Figures 14, 15, 16 and 17.

For a plant with East-West orientation it is not possible to move the reflectors using the same hourly law for $\theta_p$angle. In fact, particularly during winter operation, around the p axis the rotations of the various mirrors must be considerably different (see Figure 16). However, the trends of the θ_q angles are very similar to each other. For this type of system, in fact, it may be convenient to move the mirrors with the same motor around the q axis, differentiating the movement only around the other axis. The hourly law of θ_q becomes the following:

$$\theta_q(D) = \theta_q(D = 0) \tag{27}$$

In this case, therefore, there is no need to shift the reflectors. The errors made with this application, with reference to the summer solstice and the winter solstice, are presented in Figures 18 and 19.

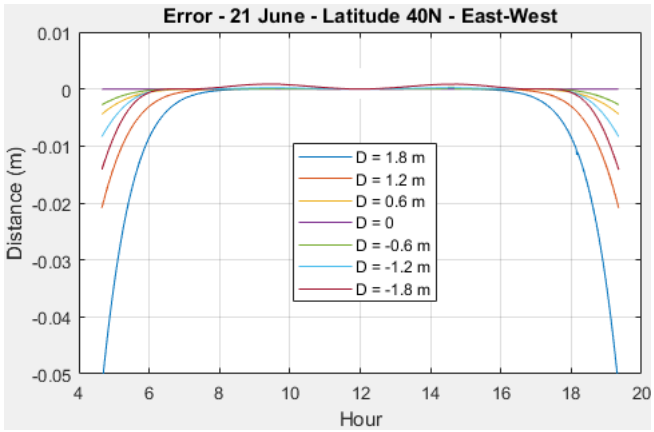

Figure 18. Tracking error- June 21 – East-West

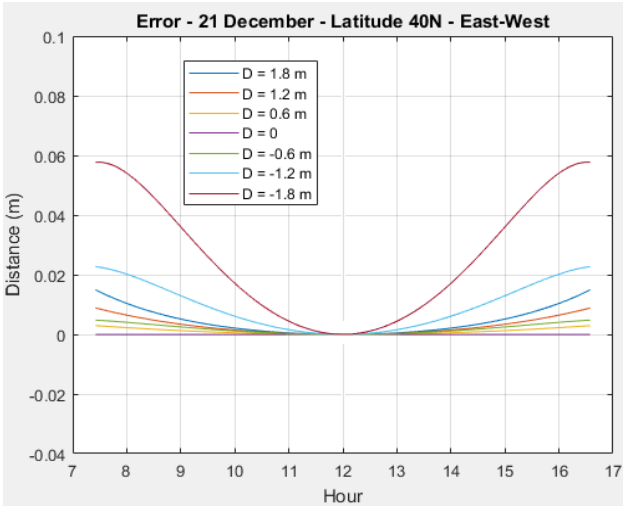

Figure 19. Tracking error- December 21 – East-West

The errors are kept below 0.06 m, so it is possible to use a secondary reflector with an aperture of about 0.12 m greater than the diameter of the tube.

Although it is possible to obtain a better tracking, the constructive application of a movement system for an East-West plant is more complex. In fact, rotations around the primary axes are made by means of independent motors; while rotations must be made with the same motor around the secondary axes (which undergo the primary rotation). It is not easy to design a kinematic system that guarantees the same rotations around axes that move independently.

Finally, an energy analysis was carried out to assess numerically the increase in performance of a system with biaxial reflectors on the ends of the collector.

The additional power that reaches the tube is:

$$P_t = \sum_{j=1}^{n} DNI \cdot \cos i \cdot k \cdot l \cdot \rho_t \cdot (\tau\alpha) \qquad (28)$$

in which:

- n is the number of primary reflectors;
- DNI is the Direct Normal Irradiance, estimated through the ASHRAE method [5];
- cos i is the angle of incidence of the j-th mirror;
- *k* is the length of pipe which, with the classical movement, would not be irradiated (see paragraph 2);
- *l* is the width of each mirror;
- ρt is the reflectivity of the mirror;
- $(\tau\alpha)$ is the effective product of the transmissivity and absorptivity of the absorber.

In the calculation examples, shown below, the recovered thermal power is compared to a traditional system with the characteristics shown in Table 1.

Table 1. Plant data

Number of rows of mirrors*n*	**9**
Absorber height *h*	3 m
Primary reflectors width *l*	0.3 m
Distance between reflectors	0.4 m
Reflectivity ρ_t	0.9
Effective product $(\tau\alpha)$	0.9

The length of the reflectors with two degrees of freedom must be at least equal to the maximum length that *k* takes during the year.

The trends of the thermal powers gained are shown, for the two solstices, for a plant with a North-South orientation (Figures 20 and 21) and for a plant with an East-West orientation (Figures 22 and 23).

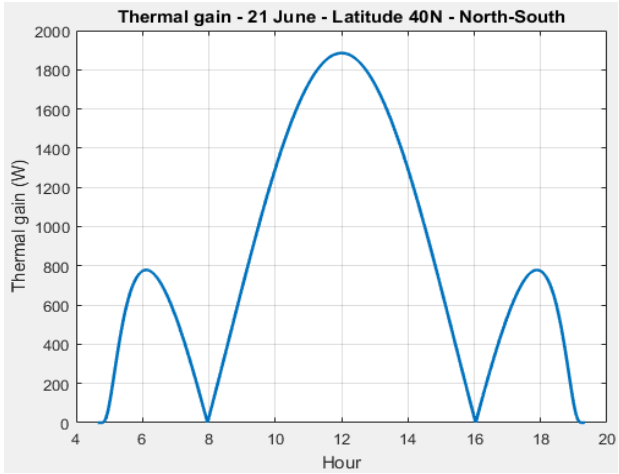

Figure 20. Thermal power- June 21 – North-South

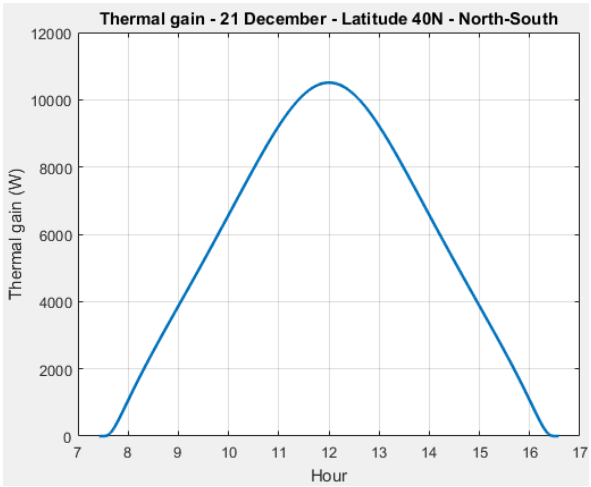

Figure 21. Thermal power- December 21 – North-South

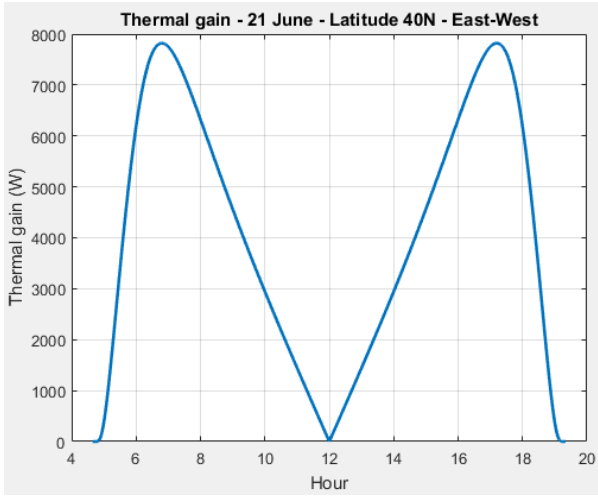

Figure 22. Thermal power- June 21 – East-West

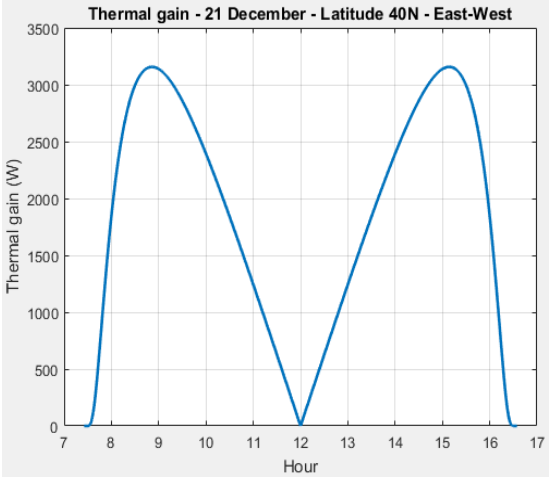

Figure 23. Thermal power- December 21 – East-West

The calculation of the integral power curves allows obtaining the numerical values of the daily thermal energy recovered (Table 2).

Table 2. Recovered thermal energy

	North-South	East-West
June 21	44.86 MJ	215.71MJ
December 21	186.48 MJ	61.13 MJ

The recovered thermal energy represents the amount of energy absorbed by the receiver tube, which would be unused in a classic Fresnel plant. The percentage increase in efficiency of the tracking system is determined by the overall length of the plant *L*. In fact, the application of this solution is advantageous especially for small plants; for plants with a long longitudinal extension, the rate recovered is marginal. What has been said is well highlighted in Figure 24 which refers to a plant whose characteristics are described in Table 1. It shows, according to the length of the plant, the percentage increase of energy absorbed by the pipe compared to a traditional linear Fresnel plant.

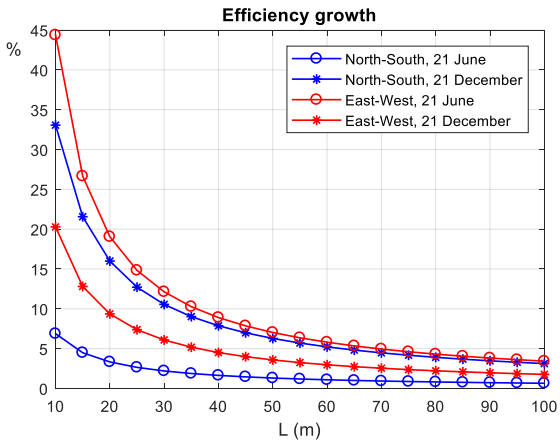

Figure 24. Increase of the tracking system efficiency according to the length of the system

6. CONCLUSIONS

Traditional linear Fresnel plants have an important geometric energy loss, attributable to the single degree of freedom with which the primary reflectors are provided.

In the present work an engineering technical solution was analysed to limit this drawback. A movement system has been proposed consisting of primary reflectors capable of rotating around two axes, to be installed at the ends of the system, orthogonally to the longitudinal axis, in order to eliminate the edge effects.

From a geometrical point of view, the orientation in space that each mirror must have in order to reflect the solar radiation at the same cross-section as the point where the reflection takes place has been determined.

This can be achieved by rotating the reflectors primarily around their longitudinal axis and secondly around their transverse axis.

In the paper, the temporal functions of both angles of rotation were determined analytically. From a purely theoretical point of view, to obtain a perfect instantaneous tracking, two independent servomotors would be needed for each mirror.

From an application point of view, to avoid an excessive increase in initial installation costs, an alternative solution has been studied, through which the mirrors are driven by the same motor in the rotation around an axis, while they have their own motor for the other rotation.

In particular, for systems oriented in the North-South direction, the same motor can be used for primary rotation, shifting the various reflectors at an appropriate angle. In order to reduce the error made with this solution, the phase shift angle must be changed at least twice a year.

On the other hand, plants with East-West orientation can adopt the same servomotor for secondary rotation, without shifting the rotation angles between them. However, in this case, the independent rotation of the secondary axes makes the installation of the motor more complicated because it is not sufficient to use a simple rack with pinions.

Lastly, the effective energy benefit obtained with this solution was estimated. For a location at a latitude of 40 ° N, more energy is recovered in the summer months with a plant with an East-West orientation and more energy in the winter months with a North-South orientation.

REFERENCES

[1] Cucumo M, Ferraro V, Kaliakatsos D, Mele M, Barci G. (2016). Performance of a fields of geothermal probes to support the air conditioning plant of a public building powered by water/water heat pumps. International Journal of Heat and Technology 34(Sp.2): S535-S544. https://doi.org/10.18280/ijht.34Sp0248

[2] Kaliakatsos D, Cucumo M, Ferraro V, Mele M, Cucumo S, Miele A. (2017). Performance of dish-stirling CSP system with dislocated engine. International Journal of Energy and Environmental Engineering 8(1): 65-80. https://doi.org/10.1007/s40095-015-0183-z

[3] Cucumo M, Ferraro V, Kaliakatsos D, Mele M, Nicoletti F. (2017). Law of motion of reflectors for a linear Fresnel plant. International Journal of Heat and Technology 35(Sp.1): S78-S86. https://doi.org/10.18280/ijht.35Sp0111

[4] Cucumo M, Ferraro V, Kaliakatsos D, Mele M, Nicoletti F. (2016). Calculation model using finite-difference method for energy analysis in a concentrating solar plant

with linear Fresnel reflectors. International Journal of Heat and Technology 34(Sp.2): S337-S345. https://doi.org/10.18280/ijht.34Sp0221

[5] Cucumo M, Ferraro V, Kaliakatsos D, Mele M. (2015). Analysis of the performances of a dish-stirling system equipped with hot chamber. International Journal of Heat and Technology 33(4): 125-136. https://doi.org/10.18280/ijht.330416

NOMENCLATURE

a	solar azimuth, rad
a_1, a_2	plane π coefficients
D	distance of the reflector from the projection of the tube on the ground, m
DNI	Direct Normal Irradiance, W.m-2
e	tracking error, m
$\hat{e}$	error angle of the reflected beam, rad
h	height of the tube, m
i	angle of incidence, rad
k	length of the unirradiated tube, m
l	width of the primary reflector, m
L	length of the plant, m
$\hat{n}$	normal versor to the primary reflector
$\hat{n}_S$	solar ray versor
$\hat{n}_t$	ideal reflection ray versor
$\hat{n}_{t,real}$	real reflection ray versor
p, q	longitudinal and transversal axes of reflector
$\hat{p}$, $\hat{q}$	versors of longitudinal and transversal axes of reflector
P_t	recovered thermal power, W
x, y, z	spatial coordinates, m

Greek symbols

(τα)	effective product transmissivity of glass and absorptivity of tube
α	solar altitude, rad
β	tilt angle of mono-axial reflector, rad
θ_a	azimuth angle of the normal to reflector, rad
θ_{ac}	correct azimuth angleof the normal to reflector, rad
θ_α	angular height of the normal to reflector, rad
θ_P	angle of rotation of reflector around the *p*-axis, degrees
θ_q	angle of rotation of reflector around the *q*-axis, degrees
π	reflection plan
ρ_t	surface reflectivity of primary reflector